

NUMERICAL MODELING OF BUOYANT TURBULENT MIXING LAYERS

AC. BENNIS*, T. CHACÓN REBOLLO†, M. GÓMEZ MÁRMOL† AND R. LEWANDOWSKI*

* IRMAR, Université de Rennes 1, Campus de Beaulieu, 35042 Rennes Cedex, France.

† Departamento de Ecuaciones Diferenciales y Análisis Numerico, Universidad de Sevilla. C/Tarfia, s/n.41080, Sevilla, Spain

Abstract

We introduce in this paper some elements for the mathematical and numerical analysis of turbulence models for oceanic surface mixing layers. In these models the turbulent diffusions are parameterized by means of the Richardson's number, that measures the balance between stabilizing buoyancy forces and un-stabilizing shearing forces. The well-posedness of these models is a difficult mathematical problem, due to the partial monotonic nature of the space operators involved. We analyze the existence and stability of equilibria state, and devise a conservative numerical scheme satisfying the maximum principle. We present some numerical tests for realistic flows in tropical seas that reproduce the formation of mixing layers, in agreement with the physics of the problem.

Key words: *Turbulent mixing layers, Richardson's number, First order closure models, Conservative numerical solution, Stability of steady states, Tests for tropical seas*

AMS subject classifications: *0123 1234*

1 Introduction

This paper is devoted to the mathematical and numerical analysis of turbulence models of surface oceanic mixing layers. The wind-stress generates intense mixing processes in a layer below the ocean surface. This layer has two parts, the upper one is an homogeneous layer, known as the mixed layer. This layer presents almost-constant temperature (and salinity). The bottom of the mixed layer corresponds to the top of the thermocline. In tropical seas a sharp thermocline is formed. Below this layer appears a thinner layer where still mixing processes do occur, but which has not a homogeneous structure. The

Research of T. Chacón and M. Gómez partially funded by Spanish DIG grants MTM2006-01275.

zone formed by the two layers is known as the mixing layer. Its thickness may vary between ten meters and a few hundred of meters, depending on the latitude. It also presents seasonal variations.

The parametrization of turbulence in the mixing layer must take into account the two forces that act in the momentum and mass exchange produced by mixing effects: Buoyancy and shear. This introduces additional complexities with respect to the usual modeling of turbulent flows with constant density, from both the physical and the mathematical standpoints. Closure terms are now parameterized in terms of the Richardson number (that measures the balance between stabilizing buoyancy forces and un-stabilizing shearing forces), that in this sense plays a role similar to that of the Reynolds number, used to parameterize closure terms for constant-density turbulence.

In this paper we introduce some mathematical and numerical elements for the analysis of the simplest turbulence models of mixing layers. These are first order closure models: Pacanowski and Philander model (called PP model, 1981, [6]) and the Large and Gent model (called KPP model, 1994, [3]) (Section 2). Let us mention that second order models have been developed by Mellor and Yamada (called MY model, 1982, [5]) and Gaspar et al. (1990,[1]). These models are widely used in physical oceanographic applications, but have received few attention from the mathematical community.

We observe that, in despite of their apparent simplicity, the well-posedness of first-order models is a difficult mathematical problem due to the partial monotonic nature of the space operators involved (Section 3). We analyze the existence of equilibria states, proving that these necessarily correspond to linear profiles of velocity and temperature (or salinity) (Section 4). We also analyze the stability of these equilibria, and prove that at least one is stable for vertical stable configurations. We introduce a new model that has just one equilibrium state (Section 5). We next devise a conservative numerical scheme for which we prove a maximum principle (Section 6). We finally present some numerical tests for realistic flows in tropical seas that reproduce the formation of mixing layers, in agreement with the physics of the problem. We stress that our new models produces results very close to the PP one, and in addition is able to handle unstable profiles (Section 7).

2 Setting of model problems

Typically, the variables used to describe the mixing layer are the statistical means of density and velocity (denoted by u and ρ). In the ocean, density =function(temperature, salinity) (State equation). We shall consider the density as an idealized thermodynamic variable.

We assume

$$U = (u(z, t), 0, w(z, t)), \quad p = p(z, t), \quad \rho = \rho(z, t)$$

and neglect Coriolis forces (hypothesis accurate for tropical oceans) and laminar diffusion (which will be absorbed by eddy diffusion). Then the averaged Navier-

Stokes equations reduce to

$$\begin{cases} \frac{\partial u}{\partial t} = -\frac{\partial}{\partial z} \langle u' w' \rangle, \\ \frac{\partial \rho}{\partial t} = -\frac{\partial}{\partial z} \langle \rho' w' \rangle, \end{cases} \quad (1)$$

To close these equations, we use the concept of eddy diffusion:

$$-\langle u' w' \rangle = \nu_1 \frac{\partial u}{\partial z}, \quad -\langle \rho' w' \rangle = \nu_2 \frac{\partial \rho}{\partial z}.$$

Coefficients ν_1 and ν_2 are expressed as functions of the **gradient Richardson number R defined as**

$$R = -\frac{g}{\rho_{ref}} \frac{\frac{\partial \rho}{\partial z}}{\left(\frac{\partial u}{\partial z}\right)^2}$$

Note that R is the ratio between the stabilizing vertical forces due to buoyancy and the un-stabilizing horizontal ones due to shear in a water column.

When $R \gg 1$, a strongly stratified layer takes place. This correspond to a stable configuration. When $0 < R \ll 1$, a slightly stratified layer takes place. This correspond to a configuration with low stability. The case $R < 0$ corresponds to a configuration statically unstable ($\frac{\partial \rho}{\partial z} > 0$), that in fact we are not modeling. However, we must handle this situation for our numerical experiments. A simple way is to set large constant values for the turbulent diffusions in this case.

The set of equations, initial and boundary conditions governing the mixing layer can now be written

$$\begin{cases} \frac{\partial u}{\partial t} - \frac{\partial}{\partial z} \left(\nu_1 \frac{\partial u}{\partial z} \right) = 0, \\ \frac{\partial \rho}{\partial t} - \frac{\partial}{\partial z} \left(\nu_2 \frac{\partial \rho}{\partial z} \right) = 0, \text{ for } t \geq 0 \text{ and } -h \leq z \leq 0, \\ u = u_b, \rho = \rho_b \text{ at the depth } z = -h, \\ \nu_1 \frac{\partial u}{\partial z} = V, \nu_2 \frac{\partial \rho}{\partial z} = Q \text{ at the surface } z = 0, \\ u = u_0, \rho = \rho_0 \text{ at initial time } t = 0. \end{cases} \quad (2)$$

Here, V is the forcing exerced by the wind-stress ($V = \frac{\rho_{air}}{\rho_{ref}} C_{friction} |U^{air}|^2$), and Q represents the thermodynamical fluxes, heating or cooling, precipitations or evaporation.

To model the turbulent diffusions in terms of the Richardson number, a central idea is that a stable configuration due to buoyancy forces inhibits the turbulent exchange of mass and momentum. Pacanowski and Philander [6] propose

$$\nu_2(R) = \frac{Constant}{(1 + \sigma R)^n} \nu_1(R).$$

This leads to the modeling $\nu_1 = f_1(R)$, and $\nu_2 = f_2(R)$, with

$$f_1(R) = \alpha_1 + \frac{\beta_1}{(1+5R)^2}, \quad f_2(R) = \alpha_2 + \frac{f_1(R)}{1+5R}, \quad \text{for PP model, and}$$

$$f_1(R) = \eta_1 + \frac{\gamma_1}{(1+10R)^2}, \quad f_2(R) = \eta_2 + \frac{\gamma_2}{(1+10R)^3} \quad \text{for KPP model.}$$

The constants are chosen to fit numerical results with experimental measurements, these are given by $\alpha_1 = 1.10^{-4}$, $\beta_1 = 1.10^{-2}$, $\alpha_2 = 1.10^{-5}$, and $\eta_1 = 1.10^{-4}$, $\gamma_1 = 1.10^{-1}$, $\eta_2 = 1.10^{-5}$, $\gamma_2 = 1.10^{-1}$ (units: m^2s^{-1}).

3 Well-posedness

Some elements for the analysis of the well-posedness of problem (2) are deduced from the analysis of monotonicity of the space operator appearing in it.

Let us assume that the functions f_i are bounded C^1 functions, with

$$f'_i(R) \leq 0, \quad (i = 1, 2). \quad (3)$$

Denote $\mathbf{v} = (\rho, u)^T$, $\mathbf{V} = (Q, V)^T$, $M = M(R) = \begin{pmatrix} f_1(R) & 0 \\ 0 & f_2(R) \end{pmatrix}$. For any function $a = a(t, z)$, we shall denote $\partial_z a = \frac{\partial a}{\partial z}$, $\partial_t a = \frac{\partial a}{\partial t}$.

Thus, our system can be written under the form (we assume homogeneous Dirichlet boundary conditions for simplicity),

$$\partial_t \mathbf{v} - \partial_z (M(R) \partial_z \mathbf{v}) = 0, \quad (4)$$

$$M(R) \partial_z \mathbf{v}|_{z=0} = \mathbf{V}, \quad \mathbf{v}|_{z=-h} = \mathbf{0}, \quad (5)$$

$$\mathbf{v}|_{t=0} = \mathbf{v}_0. \quad (6)$$

Let now $A = A(\mathbf{v})$ and \mathbf{F} be defined by

$$\begin{aligned} (A(\mathbf{v}), \mathbf{w}) &= \int_{-h}^0 M(R) \partial_z \mathbf{v} \cdot \partial_z \mathbf{w} = (M(R) \partial_z \mathbf{v}, \partial_z \mathbf{w}), \\ (\mathbf{F}, \mathbf{w}) &= \mathbf{V} \cdot \mathbf{w}(0). \end{aligned}$$

Therefore system (4) – (5) – (6) is a system of the form

$$\frac{d\mathbf{v}}{dt} + A(\mathbf{v}) = \mathbf{F}, \quad \mathbf{v}(0) = \mathbf{v}_0,$$

in the sense that $\forall \mathbf{w} \in H^2$

$$\frac{d}{dt} (\mathbf{v}, \mathbf{w}) + (A(\mathbf{v}), \mathbf{w}) = (\mathbf{F}, \mathbf{w})$$

where the space H is defined by $H = \{u \in H^1([-h, 0]), \quad u(-h) = 0\}$.

We want to use the theory of monotonic operators to analyze the well-posedness of this equation. We intend to prove that the operator A is monotonic, in the sense that

$$\forall (\mathbf{v}_1, \mathbf{v}_2) \in H^{2 \times 2}, \quad (A(\mathbf{v}_1) - A(\mathbf{v}_2), \mathbf{v}_1 - \mathbf{v}_2) \geq 0.$$

In the actual stage of our research, we are able to prove that under condition (3) indeed we have

$$\forall (\mathbf{v}_1, \mathbf{v}_2) \in H^2 \times H^2, \quad (A(\mathbf{v}_1) - A(\mathbf{v}_2), \mathbf{v}_1 - \mathbf{v}_2) \geq C_K \|\partial_z \mathbf{v}_1 - \partial_z \mathbf{v}_2\|_{L^2(-h,0)}^2, \quad (7)$$

if $\mathbf{v}_1, \mathbf{v}_2$ belong to a neighborhood K of the origin. We hope that this will allow to prove a well-posedness result for small data.

4 Equilibria states

Although we are not able to analyze the model system (2) in general, it is possible to study some properties of equilibria states. Let us consider the stationary model system:

$$\frac{\partial}{\partial z} \left(f_1(R) \frac{\partial u}{\partial z} \right) = 0, \quad \frac{\partial}{\partial z} \left(f_2(R) \frac{\partial \rho}{\partial z} \right) = 0. \quad (8)$$

Integrating (8) with respect to z we obtain

$$\begin{cases} f_1(R) \frac{\partial u}{\partial z} = \text{constant} = V & \text{(momentum flux),} \\ f_2(R) \frac{\partial \rho}{\partial z} = \text{constant} = Q & \text{(heat flux).} \end{cases} \quad (9)$$

Using the expression (2), we deduce an **implicit equation** for R

$$R = -\frac{g}{\rho_0} \frac{Q}{V^2} \frac{(f_1(R))^2}{f_2(R)}$$

If this equation has a solution R^e , this reads

$$\frac{\text{Potential energy}}{\text{Turbulent kinetic energy}}(\text{Equilibrium}) = \frac{-Q}{V^2} \times \text{Constant}(R^e).$$

Note that from (9), the equilibria states are linear profiles for both velocity and density.

PP and KPP models present **several equilibria** R^e for a range $[r^*, +\infty)$ of fluxes ratio $r = -Q/V^2$, where r^* is negative. This corresponds to static instability. So, these model include as mathematical equilibria some physical static unstable configurations.

To avoid the multiplicity of steady states, we introduce a new model, given by

$$f_1(R) = \alpha_1 + \frac{\beta_1}{(1+5R)^2}, \quad f_2(R) = \alpha_2 + \frac{f_1(R)}{(1+5R)^2},$$

with the same constants as the PP model. This new model has a **unique equilibrium** R^e for any fluxes ratio r . This is a mathematically favorable property, still without physical meaning when $r < 0$.

5 Stability of equilibria states

We analyze the linear stability of equilibria states. To do it, we construct a model of time evolution of a small perturbation of a equilibrium state (u^e, ρ^e) :

$$(u, \rho) = (u^e, \rho^e) + (u', \rho')$$

Set $\psi = \frac{\partial \rho}{\partial z}$ and $\theta = \frac{\partial u}{\partial z}$, and so $R = R(\theta, \psi)$, $\nu_i = \nu_i(\theta, \psi)$. The equations satisfied by the perturbation (u', ρ') are deduced from model equations :

$$\begin{cases} \frac{\partial u'}{\partial t} - \frac{\partial}{\partial z} (\nu_1(\theta, \psi) (\theta^e + \theta')) = 0, \\ \frac{\partial \rho'}{\partial t} - \frac{\partial}{\partial z} (\nu_2(\theta, \psi) (\psi^e + \psi')) = 0. \end{cases} \quad (10)$$

The linearized equations for (u', ρ') then are

$$\frac{\partial V}{\partial t} - A \frac{\partial^2 V}{\partial z^2} = 0, \text{ with } V = \begin{pmatrix} u' \\ \rho' \end{pmatrix}, \quad (11)$$

where A is the **amplification matrix**,

$$A = \begin{pmatrix} \nu_1^e + \theta^e \left(\frac{\partial \nu_1}{\partial \theta} \right)^e, & \theta^e \left(\frac{\partial \nu_1}{\partial \psi} \right)^e \\ \psi^e \left(\frac{\partial \nu_2}{\partial \theta} \right)^e, & \nu_2^e + \psi^e \left(\frac{\partial \nu_2}{\partial \psi} \right)^e \end{pmatrix}.$$

Linear stability of the equilibrium solution (u^e, ρ^e) follows if any perturbation (u'_0, ρ'_0) imposed at initial time $t = 0$ is damped as $t \rightarrow \infty$. This is verified if the eigenvalues λ_1, λ_2 of A are such that $Re(\lambda_1) > 0$ and $Re(\lambda_2) > 0$. After some algebra, we conclude that all models are linearly stable for $R^e > 0$. But strikingly also for a small range $[R^*, 0]$ with $R^* < 0$, which (we recall) corresponds to physically unstable configurations.

We have also investigated the non-linear stability of our models. To do it, we have solved numerically the full non-linear system (2) starting from small and even large perturbations of equilibria states. We have used the numerical scheme described in the next section. Our conclusions also are that for all models the equilibria states are non-linearly stable, and, even more, behave as strong attractors. The typical time that a given initial state takes to approach an equilibrium state is of the order of several months. This must be compared with the typical time of formation of the thermocline, which is of a few days.

6 Numerical discretization

We have performed a centered conservative semi-implicit discretization of the PDEs appearing in model (2) by finite differences. To describe it, assume that the interval $[-h, 0]$ is divided into N subintervals of length $\Delta z = h/(N-1)$, with nodes $z_i = -(i-1)h\Delta z$, $i = 1, \dots, N$. We respectively approximate the values $u(z_i, t_n)$, $\rho(z_i, t_n)$ by u_i^n and ρ_i^n , where $t_n = n\Delta t$. The equation for u , for instance, is discretized at node z_i , with $i = 2, \dots, N-1$ by

$$\frac{u_i^{n+1} - u_i^n}{\Delta t} - \frac{f_1(R_{i-1/2}^n)u_{i-1}^{n+1} - \left[f_1(R_{i-1/2}^n) + f_1(R_{i+1/2}^n) \right] u_i^{n+1} + f_1(R_{i+1/2}^n)u_{i+1}^{n+1}}{(\Delta z)^2} = 0,$$

where

$$R_{i-1/2}^n = -\frac{g}{\rho_{ref}} \frac{(\rho_i^n - \rho_{i-1}^n)/\Delta z}{[(u_i^n - u_{i-1}^n)/\Delta z]^2},$$

and a similar discretization for the equation for ρ . The boundary conditions have been discretized by

$$u_1^{n+1} = u_b^{n+1}, \quad \rho_1^{n+1} = \rho_b^{n+1};$$

$$f_1(R_{N-1/2}^n) \frac{u_N^{n+1} - u_{N-1}^{n+1}}{\Delta z} = V_N^{n+1}.$$

This last equation allows to compute u_N^{n+1} from u_{N-1}^{n+1} . So we may construct our discretization in terms of the unknowns $U^{n+1} = (u_2^{n+1}, \dots, u_{N-1}^{n+1})$ and similarly for ρ . In matrix form, this discretization reads

$$A^{n+1} U^{n+1} = B^{n+1},$$

where A^{n+1} and B^{n+1} respectively are the tridiagonal matrix and the vector array defined with obvious notation by

$$A_{i-1,i}^{n+1} = -\alpha_{i-1/2}^n, \quad A_{i,i}^{n+1} = 1 + \alpha_{i-1/2}^n + \alpha_{i+1/2}^n, \quad A_{i+1,i}^{n+1} = -\alpha_{i+1/2}^n, \quad i = 2, \dots, N-2;$$

$$A_{N-2,N-1}^{n+1} = -\alpha_{N-3/2}^n, \quad A_{N-1,N-1}^{n+1} = 1 + \alpha_{N-3/2}^n;$$

$$B^{n+1} = (u_2^n + \alpha_{3/2}^n u_b^n, u_3^n, \dots, u_i^n, \dots, u_{N-2}^n, u_{N-1}^n + \frac{\Delta t}{\Delta z} V)^t,$$

where

$$\alpha_{i-1/2}^n = \frac{\Delta t}{(\Delta z)^2} f_1(R_{i-1/2}^n).$$

As $f_1 \geq 0$, A^{n+1} is an M-matrix and then $(A^{n+1})^{-1}$ has positive entries. Then, we deduce a *maximum principle*: If the initial data, u_b^n and V are positive, the u_i^n are all positive.

7 Numerical tests

We have simulated some realistic flows, corresponding to the Equatorial Pacific region called the West-Pacific Warm Pool, located at the equator between $120^\circ E$ and $180^\circ E$. In this region the sea temperature is high and almost constant along the year ($28-30^\circ C$). The precipitations are intense and hence the salinity is low. We initialize the code with data from the TAO (Tropical Atmosphere Ocean)

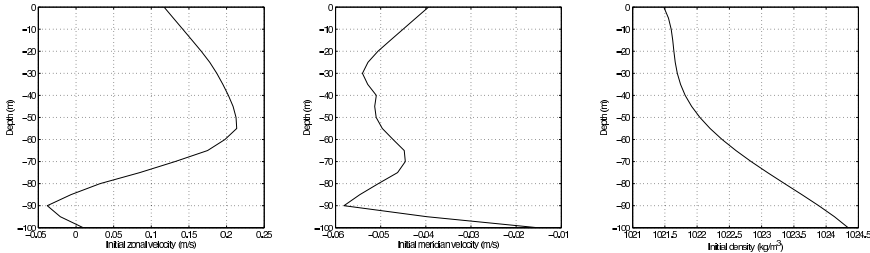


Figure 1: Initial zonal velocity, meridian velocity and density profiles (from left to right).

array (McPhaden [4]), which have been used in many numerical simulations.

Here, we present the results corresponding to a mixed layer induced by the wind stress, using initial velocity and density profiles measured at $0^\circ N, 165^\circ E$ for the time period between the 15th June 1991 and the 15th July 1991, displayed in Figure 1. Observe that the density profile does not present a mixed layer.

We used a two-dimensional version of model (2), with buoyancy flux equal to $-1.10^{-6} kg.m^{-2}.s^{-1}$ ($\simeq -11 W/m^2$), which is realistic for this region (Cf. [2]). We have taken as boundary conditions, a zonal wind (u_1) equal to $8.1 m/s$ (eastward wind) and a meridional wind (u_2) equal to $2.1 m/s$ (northward wind). These values are larger than the measured ones, because we want to force the formation of a mixed layer. We have used $\Delta z = 1m$ and $\Delta t = 60s$. The results are grid-independent, in the sense that they remain practically unchanged when Δz and Δt decrease.

Figure 2 displays the results corresponding to $t = 48$ hours. On top we represent the whole mixing layer, and on bottom, the upper 40m of layer. The plots for density profiles show the formation of a pycnocline at $z = -30$, approximately. Velocity and density profiles are quite close for PP and the new model, while the velocity provided by KPP model is somewhat different, mainly near the surface. Also, the density profiles and the pycnocline simulated by the three models are quite similar.

Let us remark that our new model is the one that introduces the smallest levels of turbulent viscosity and diffusion. It is also able to simulate non-stable initial profiles, providing physically coherent results.

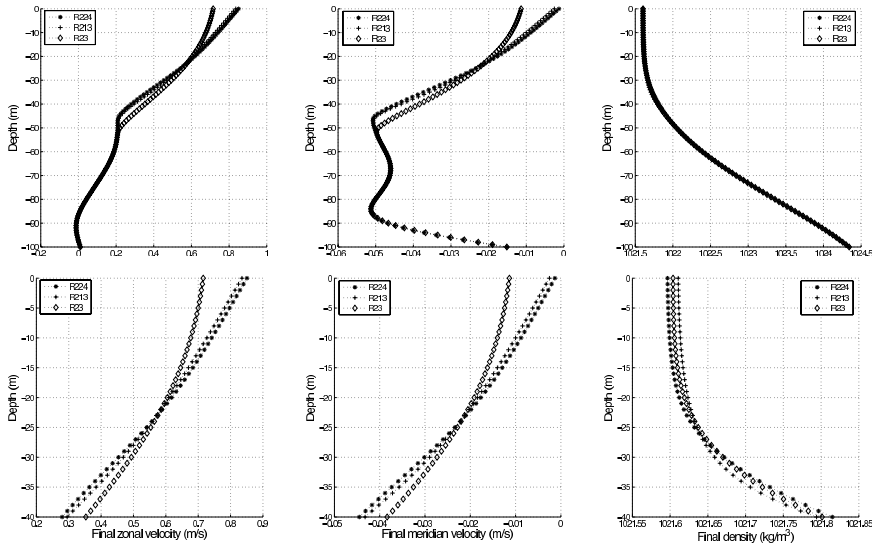


Figure 2: Comparison of three turbulence models: R213 (PP), R224 (KPP), R23 (new one) (In this notation R_{ijk} , i , j and k represent the exponents of the denominators in the definition of the turbulent diffusions f_1 and f_2). Top: Full mixing layer. Bottom: Upper 40m of mixing layer.

References

- [1] P. Gaspar, Y. Gregoris and L. J. M. A simple eddy kinetic energy model for simulations of oceanic vertical mixing: test at station papa and long-term upper ocean study site. *J. Geophys. Research.* Vol 16, 179-193. 2001.
- [2] P. R. Gent. The heat budget of the toga-coare domain in an ocean model. *J. Geophys. Res.* Vol 96, 3323-3330. 1991.
- [3] W. G. Large, C. McWilliams and S. C. Doney. Oceanic vertical mixing: a review and a model with a non-local boundary layer parametrization. *Rev. Geophys.* Vol. 32, 363-402. 1994
- [4] M. McPhaden. The tropical atmosphere ocean (tao) array is completed. *Bull. Am. Meterorol. Soc.* Vol. 76, 739-741. 1995.
- [5] G. Mellor and T. Yamada. Development of a turbulence closure model for geophysical fluid problems. *Reviews of Geophysics and Space Physics.* Vol. 20, 851-875. 1982.
- [6] R. C. Pacanowski and S. G. H. Philander. Parametrization of vertical mixing in numerical models of the tropical oceans. *J. Phys. Oceanogr.* Vol 11, 1443-1451. 1981.